

Study of some simple ferrites as reducing gas sensors

F. TUDORACHE*, E. REZLESCU, P. D. POPA, N. REZLESCU

National Institute of Research and Development for Technical Physics-IFT, No. 47, Blvd. D. Mangeron, 700050 Iasi, Romania

Four spinel ferrites, MFe_2O_4 ($M = Cu, Cd, Zn$ and Ni), having various grain sizes (100 – 700 nm) were prepared by sol-gel-selfcombustion and their sensing properties to reducing gases were investigated. The gas sensing characteristics were obtained by measuring the sensitivity as a function of various controlling factors, like operating temperature, composition and concentration of the gas, and finally the response time. The sensitivity of four ferrites to reducing gases like acetone, ethanol and LPG was been compared. It was revealed that $CuFe_2O_4$ is the most sensitive to LPG and $ZnFe_2O_4$ can be used as a sensor to selectively detect ethanol vapors in air. The strong interaction between ethanol and porous $ZnFe_2O_4$ can explain the selective sensitivity to ethanol and negligible sensitivity to the other reducing gases.

(Received April 1, 2008; accepted June 30, 2008)

Keywords: Gas sensor, Semiconducting materials, Structure characteristics, Sensitivity, Reducing gas

1. Introduction

There is an increasing interest in the finding new materials in order to develop high performance solid state gas sensors. Semiconductor metal oxide sensors are an alternative for non expensive and robust detection systems. Spinel-type oxide semiconductors with formula MFe_2O_4 have been reported to be sensitive materials to both oxidizing and reducing gases. Liu et al [1] reported the high sensitivity of $CdFe_2O_4$ to ethanol vapor, Reddy et al [2] investigated $NiFe_2O_4$ as sensor to detect Cl_2 in air. Chen et al [3] revealed that $MgFe_2O_4$ and $CdFe_2O_4$ are sensitive and selective to liquefied petroleum gas (LPG) and C_2H_2 . Our earlier investigations [4] indicated the promoting effect of Sn ions on the improving the sensitivity of Mg ferrite to acetone gas. The tin in $MgFe_2O_4$ facilitates the oxidation of reducing gas and the occurrence of the oxygen vacancies changing the electrical conductivity. The sensing mechanism of the reducing gases consists in the change of the electrical conductivity resulting from chemical reaction between the gas molecules and adsorbed oxygen onto the metal oxide surface [5, 6].

Taking into account that the sensing phenomena mainly takes places on the material surface, the surface morphology has an essential role on the sensitivity of solid state sensor. In the last years, the nanograin materials offer new opportunities for enhancing the properties and performances of gas sensors. Several research reports [7 - 10] have confirmed the beneficial effect of nanostructure on the sensor performance.

In this paper, nanopowders of the simple spinel ferrites, $CuFe_2O_4$, $ZnFe_2O_4$, $NiFe_2O_4$ and $CdFe_2O_4$ were prepared by a method, sol-gel-selfcombustion [11]. The advantage of this method is that it enables the economic manufacture of a wide range of ceramic nanopowders and the particle size can be controlled by subsequent heat treatments [12]. Also, in this technology, solid state

reaction forms separated nanoparticles. The obtained nanopowders were tested for sensing properties to three reducing gases: liquefied petroleum gas (LPG), ethanol (C_2H_5OH) and acetone (CH_3COCH_3). It was concluded that the gas sensitivity considerably depends on the ferrite composition and the gas type to be detected.

2. Experimental

Spinel ferrites of composition MFe_2O_4 ($M = Cu, Cd, Ni$ and Zn) were prepared by sol-gel-selfcombustion. The powders of $Fe(NO_3)_3 \cdot 9H_2O$, $Cu(NO_3)_2 \cdot 3H_2O$, $Cd(NO_3)_2 \cdot 4H_2O$, $Ni(NO_3)_2 \cdot 6H_2O$, $Zn(NO_3)_2 \cdot 6H_2O$, were weighed in the desired proportions and dissolved in small amounts of distilled water. Alcohol polyvinyl was added to make a colloidal solution. By adding NH_4OH solution, the pH was adjusted to about 8 and the result was a sol of metal hydroxides and ammonium nitrate. After heating at $120^\circ C$, for 12 hours, the dried gel was ignited in a corner. The combustion wave spontaneously propagates and converts the gel into a loose powder containing very fine crystallites. All residual organic compounds were eliminated by heating the powder at $500^\circ C$ for one hour. Then, the combusted powder was compacted into pellets (cylindrical discs), of about 2 mm thickness and 7 mm diameter, at a pressure of 100 MPa. These pellets were treated at $1000^\circ C$ for 30 minutes to facilitate solid state sintering followed by furnace cooling of the samples. The structure analysis of the heat treated compacts was done by X-ray diffraction (CoK α radiation) using DRON-2 type diffractometer. The surface morphology was analyzed using a scanning electron microscope (Tesla-BS340). The grain size was appreciated from SEM micrographs. Bulk density was determined from the dimensions and mass. The specific surface area was determined using equation [13, 14]

$$A = \frac{s}{v \cdot d} = \frac{6}{d \cdot D_m}, \quad (1)$$

were s and v are the particle surface and volume respectively, d is the bulk density and D_m is the average grain size. The number 6 is the shape factor. It is assumed that the particles of a specimen have the same size and the same shape.

For electric measurement, two silver electrodes were applied on a face of the ferrite disc, as in Figure 1.

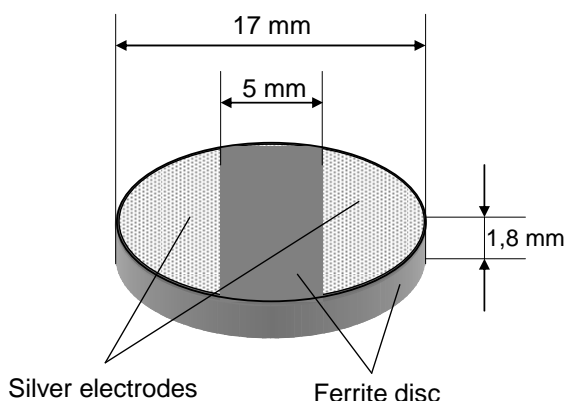


Fig. 1. Design of ferrite sensor with silver electrodes

The electrical resistance was measured by a two-point method with a digital LCR meter at 100 Hz. For gas sensing measurements, the sensor element (ferrite disc) was provided with a heater and the assemble heater-sensor element was introduced in a glass chamber (2 dm^3). The test gases were injected with a syringe into the glass chamber. The measurements were done in the temperature range from 150°C to 400°C . A cromel-alumel thermocouple located in close proximity of the sensor element was used to measure the working temperature.

The resistance of the ferrite sensor placed into the measuring chamber was measured at fixed temperatures, both in air and in the presence of the test gas. The sensitivity S was calculated with the relation

$$S = \frac{\Delta R}{R_a} = \frac{R_a - R_g}{R_a}, \quad (2)$$

were R_a is the ferrite resistance in air and R_g is the resistance in the test gas at a given temperature. Taking into account the thermal inertia of ferrites, all measurements were carried out under the thermal stabilization conditions. All data were collected at least 30 minutes after gas exposure. After each change of the test gas, the sensor element was activated by submitting it to

heat treatment at 500°C for 5 minutes in order to form the initial structure and its thermodynamically stabilize. Heat cleaning of the samples was found to be necessary for better and reproducible sensitivity.

3. Results and discussion

3.1. Structure characterization

By X-ray diffraction it was confirmed the formation of cubic spinel structure in all samples annealed at 1000°C . SEM micrographs on the four ferrite compositions are shown in Figure 2. SEM images were made before exposing to test gases. Each ferrite is characterized by a porous structure and submicron grains. The porosity is entirely intergranular, the pores are interconnected to form pore channels. Since the pores are channeled and do not have well-defined shape, it is difficult to give a particular dimension of the pores.

It is evident that the morphology is dependent on the ferrite composition. Though all samples were prepared under identical conditions, the crystallite size was not the same for all ferrites. This is probably due to different rate of the solid state cation diffusion during the sintering. Also, all ferrites, except for CuFe_2O_4 , have rounded grains and a homogeneous grain size distribution, between 100 and 300 nm.

The structural characteristics are summarized in Table 1. The main conclusion from Table 1 is that a decrease in grain size results in an increase in specific surface area and porosity. Among the investigated ferrites, ZnFe_2O_4 is characterized by the smallest grain size, 100 nm, and the highest porosity, 48.4 %, that imply a much more active surface towards test gases. But CuFe_2O_4 exhibits large faceted crystallites (700 nm) and the smallest surface area ($2.4 \text{ m}^2/\text{g}$).

Table 1. Structural characteristics for the studied ferrites

Ferrite	Bulk density d (g/cm^3)	Porosity p (%)	Average grain size D_m (nm)	Surface specific area A (g/m^3)
CuFe_2O_4	3.6	32.8	700	2.4
CdFe_2O_4	3.3	45.5	300	6.0
NiFe_2O_4	3.5	35.2	200	8.6
ZnFe_2O_4	2.7	48.4	100	22.2

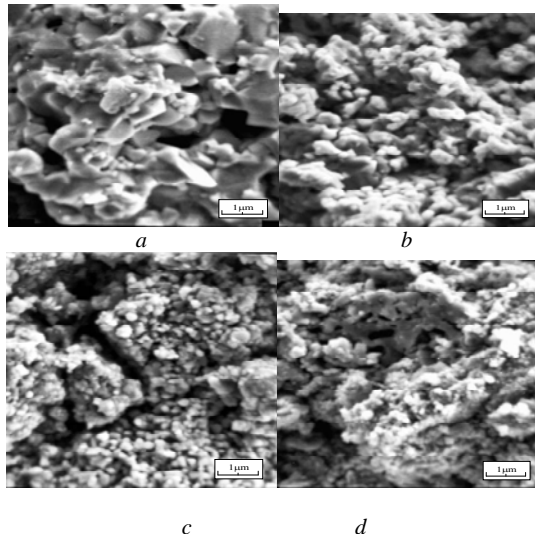


Fig. 2. SEM micrographs of the CuFe_2O_4 (a), CdFe_2O_4 (b), NiFe_2O_4 (c) and ZnFe_2O_4 (d) ferrites. Enlargement x8000

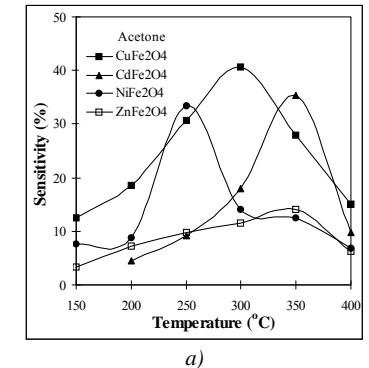
3.2. Gas sensing properties

Figure 3 (a, b and c) illustrates the gas sensitivities of the four simple ferrites as a function of operating temperature, towards acetone, ethanol and LPG vapors. At least three samples of each ferrite composition were tested, but in all figures are shown the results for only one sensor from each ferrite type, since no large difference between the sensors of the same ferrite type was observed. All sensitivity measurements was performed at temperatures higher than 150°C . At lower temperatures the electrical response to the test gases was reduced. Therefore, elevated temperatures are required to change the oxidation state and conductance of ferrite. From Figure 3 one can remark two observations:

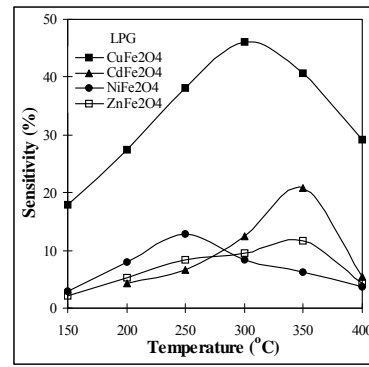
i) Each of the curves shows a maximum of the sensitivity corresponding to an optimum operating temperature of the sensor element. For CdFe_2O_4 and ZnFe_2O_4 the sensitivity maximum appears at 350°C , for CuFe_2O_4 it appears at 300°C and for NiFe_2O_4 at 250°C . Therefore, the ferrite sensors have need of thermal excitation to response to the investigated gases and the best response can be obtained if each sensor operates at its optimum working temperature.

ii) There are large differences in the sensitivity values to various gases of the four ferrites. CuFe_2O_4 shows an exceptional sensitivity to LPG (Figure 3c). ZnFe_2O_4 shows considerable sensitivity to alcohol (Fig.3 b) and poor response to acetone (Figure 3a) and LPG (Figure 3c). CdFe_2O_4 is sensitive to alcohol (Figure 3b) and acetone (Figure 3a) and less sensitive to LPG (Figure 3c).

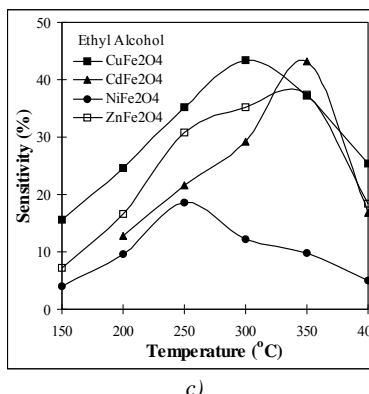
The sensitivities of the four ferrites towards the three reducing gases are compared in Figure 4. Here, the sensitivity values correspond to the optimized working temperatures for each ferrite sensor.



a)



b)



c)

Fig. 3. The sensitivity of the four simple ferrites to acetone (a), alcohol (b) and LPG (gas concentration: 150 ppm).

An interesting result is that CuFe_2O_4 element has the best sensitivity to the three reducing gases, even though this ferrite has the largest granulation and the smallest porosity (Table 1). An explanation for the high sensitivity and low selectivity of CuFe_2O_4 would be the formation of Cu^{1+} ions during the reducing gas oxidation. We recall that the electrical conduction in ferrites is mainly attributed to the electron hopping between Fe^{2+} and Fe^{3+} ions distributed on the octahedral (B) sites in the spinel structure [15]. In the inverse spinel CuFe_2O_4 , Cu^{2+} ions prefer octahedral sites. The occurrence of the Cu^{1+} ions on

the octahedral sites can provide a greater number of hoppings ($\text{Fe}^{2+} \leftrightarrow \text{Fe}^{3+}$, $\text{Cu}^{1+} \leftrightarrow \text{Cu}^{2+}$) on B sites and thus, an increase of the conduction.

On the other hand, one can remark from Figure 3 and Figure 4 that all ferrites, except for NiFe_2O_4 , have good sensitivity to ethanol. According to Ferreira et al. [16], this improved sensitivity to ethanol can be attributed to the involvement of the hydroxyl group OH^- which can react with lattice oxygen, generating the electrons for conduction. NiFe_2O_4 ferrite exhibits a selective sensitivity to acetone (Figure 4), but its acetone sensitivity is smaller than that of CuFe_2O_4 and CdFe_2O_4 ferrites.

ZnFe_2O_4 ferrite shows not only enhanced sensitivity to ethanol ($\text{C}_2\text{H}_5\text{OH}$) but also very high selectivity by the decreasing its sensitivity to LPG and acetone (Figure 4). The sensitivity to ethanol of ZnFe_2O_4 ferrite is approximately three times larger than the one to LPG or acetone.

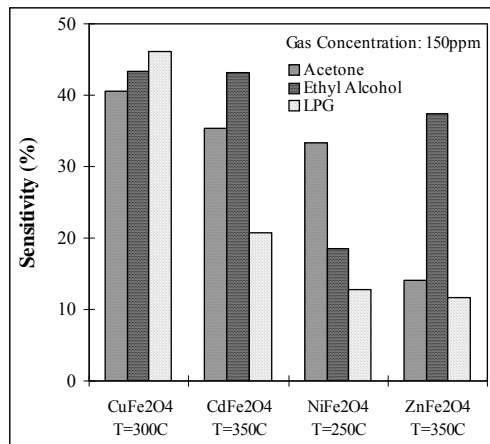


Fig. 4 Bar diagram for sensitivity of four ferrites to reducing gases

These results suggest that this ferrite may use for fabrication of ethanol vapor detector, but its high operating temperature, of 350°C , is not favorable from commercial point of view. The existence of a strong interaction between ethanol molecules and ferrite components can explain the surprising high selective sensitivity to ethanol and negligible sensing to the acetone and LPG. This high ethanol selectivity of ZnFe_2O_4 without using a catalyst is one of the characteristics of ultrafine particle ferrite and additional investigations are required to clarify this problem.

Figure 5 illustrates the behavior of the sensitivity of ZnFe_2O_4 as a function of stepwise increasing gas concentration (LPG, ethanol and acetone) from 0 to 150 ppm, at 350°C . For low gas concentrations (50–100 ppm) the sensitivity increases almost linear with gas concentration. For higher gas concentrations (over 100 ppm) the sensitivity tends to a constant value. The sensitivity largely depends on the gas type. This is remarkably higher to ethanol. The sensitivity to ethanol in 100 ppm environment is 0.35 whereas to acetone and LPG

is of about 0.1. The same measurements were repeated after one month, but the results were reproducible within the deviation limits of $\pm 5\%$.

These results demonstrate that the simple ferrite ZnFe_2O_4 is sensitive and selective for the detection of ethanol.

Figure 6 shows the plot of the response characteristics to ethanol and LPG vapors for ZnFe_2O_4 and CuFe_2O_4 sensors, respectively.

Figure 6 shows the plot of the response characteristics to ethanol and LPG vapors for ZnFe_2O_4 and CuFe_2O_4 sensors, respectively. The response time required for the sensitivity to attain 90% of its maximum value is of about 3 minutes for CuFe_2O_4 and 2 minutes for ZnFe_2O_4 , whereas the recovery time during the sensitivity fallen to 10% of its maximum value is longer, of about 4 minutes for the two ferrites. The faster response of ZnFe_2O_4 material is explained by its high porosity and finest granulation (see Figure 2d). The response and recovery times of the sensors towards other gases showed similar results and therefore these are not shown here.

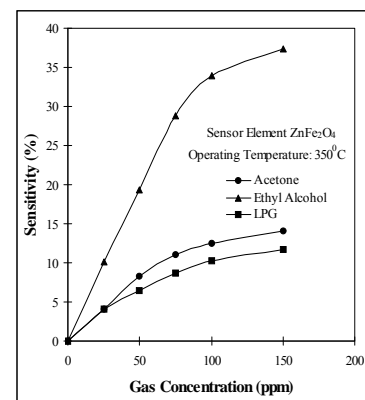


Fig.5 Sensitivity versus gas concentration of ZnFe_2O_4 sensor element

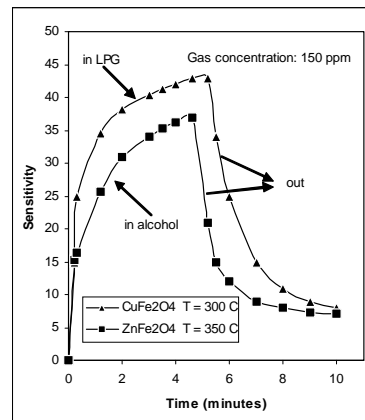


Fig.6 Response characteristics to ethanol and LPG for CuFe_2O_4 and ZnFe_2O_4 ferrites

4. Conclusions

CuFe_2O_4 , CdFe_2O_4 , ZnFe_2O_4 and NiFe_2O_4 ferrites were prepared by sol-gel-selfcombustion technology and tested for sensing properties to ethanol, LPG and acetone. SEM micrographs show a porous structure and submicronic grains, between 100 and 700 nm.

By sensitivity measurements it was found that CuFe_2O_4 has an improved sensitivity to all reducing gases at optimum working temperature of 300°C . The improved sensitivity of CuFe_2O_4 can not be explained by changes in morphology. ZnFe_2O_4 , having the highest porosity and the largest surface area, is sensitive to ethanol only. A probable explanation for selective sensitivity to ethanol and negligible sensitivity to other gases can be the strong interaction between ethanol molecules and spinel ferrite.

From present work one can conclude that CuFe_2O_4 can be used for LPG sensing, ZnFe_2O_4 and CdFe_2O_4 for ethanol sensing and NiFe_2O_4 for acetone.

These results are preliminary. Further studies aim at the improving of sensor's performance characteristics with respect to: sensitivity, response time, durability and to establish the exact role of Cu ion in the sensing mechanism of CuFe_2O_4 . Mössbauer studies would be beneficial in observing the change in the state of Cu ion in the presence or absence of reducing gases.

References

- [1] X.Q. Liu, Z.L. Xu, Y.S. Shen, A new type ethanol sensing material on CdFe_2O_4 semiconductor, *J. Yunnan Univ.* **19**, 147-149 (1997).
- [2] C. V. G. Reddy, S. V. Manorama and V. J. Rao, Semiconducting gas sensor for chlorine based on inverse spinel nickel ferrite, *Sensors and Actuators B* **55**, 90-95 (1999).
- [3] N. S. Chen, X. J. Yang, E. S. Liu and J. L. Huang, Reducing gas-sensing properties of ferrite compounds MFe_2O_4 ($\text{M} = \text{Cu, Zn, Cd, Mg}$), *Sensors and Actuators B* **66**, 178-180 (2000).
- [4] N. Rezlescu, C. Doroftei, E. Rezlescu and P. D. Popa, The influence of Sn^{4+} and/or Mo^{6+} ions on the structure, electrical and gas sensing properties of Mg-ferrite, *Physica Status Solidi A* **203**, 306-316 (2006).
- [5] A. Gurlo, N. Barsan and U. Weimar, Mechanism of NO_2 Sensing on SnO_2 and In_2O_3 Thick Film Sensors as Revealed by Simultaneous Consumption and Resistivity Measurements, in The 16th European Conference on Solid-State Transducers, Prague, Czech. Republic, 15-18 September 2002, 970-973.
- [6] T. G. G. Maffeis et al., Nano-crystalline SnO_2 gas sensor response to O_2 and CH_4 at elevated temperature investigated by XPS, *Surface Science* **520**, 29-34 (2002).
- [7] R. Rella, P. Siciliano, S. Capone, M. Epifani, L. Vasanelli and A. Liciulli, Air quality monitoring by means of sol-gel integrated tin oxide thin films, *Sensors and Actuators B* **58**, 283-288 (1999).
- [8] M. Ferroni, D. Boscarino, E. Comini, D. Gnani, G. Martinelli, P. Nelli, V. Rigato and G. Sberveglieri, Nanosized thin films of tungsten-titanium mixed oxides as gas sensors, *Sensors and Actuators B* **58**, 289-294 (1999).
- [9] R. Martins, E. Fortunato, P. Nunes, I. Fereira, and A. Marques, Zinc oxide as an ozone sensor, *Journal of Applied Physics* **96**, 1398-1408 (2004).
- [10] N. Rezlescu, N. Iftimie, E. Rezlescu, C. Doroftei, P. D. Popa, Semiconducting gas sensor for acetone based on the grained nickel ferrite, *Sensors and Actuators B* **114**, 427-432 (2006).
- [11] P. D. Popa, N. Rezlescu, A new method for preparing $\text{BaFe}_{12}\text{O}_{19}$ ferrite powder, *Romanian Reports in Physics* **52**, 769-773 (2000).
- [12] L. Cukrov, P. McCormick, K. Galatsis, W. Wlodarski, Gas sensing properties of nanosized tin oxide synthesised by mechanochemical processing, *Sensors and Actuators B* **77**, 491-495 (2001).
- [13] C. Laberty, P. Alphonse, J. J. Demai, C. Sarada, A. Rousset, *Materials Research Bulletin* **32**, 249-261 (1997).
- [14] S. Lowell, J. E. Shields, M. A. Thomas, and M. Thommes, *Characterization of Porous Solids and Powders: Surface Area, Pore Size and Density*, Kluwer Academic Publishers, Dordrecht/Boston/London 2003.
- [15] J. Smit et H. P. J. Wijn, *Les Ferrites*, Dunod, Paris 1961.
- [16] I. Ferreira, R. Igreja, E. Fortunato and R. Martins, Porous a/nc-Si: H films produced by HW-CVD as ethanol vapour detector and primary fuel cell, *Sensors and Actuators B* **103**, 344-349 (2004).

*Corresponding author: florin@phys-iasi.ro